



## Propagation from meteorological to hydrological drought in the Horn of Africa using both standardized and threshold-based indices

Rhoda A. Odongo<sup>1</sup>, Hans De Moel<sup>1</sup>, and Anne F. Van Loon<sup>1</sup>

<sup>1</sup>Institute of Environmental Studies, Vrije Universiteit Amsterdam, Netherlands

5

*Correspondence to:* Rhoda A. Odongo (rhodaachieng.odongo@vu.nl)

### Abstract

There have been numerous drought propagation studies in data-rich countries, but not much has been done for data-poor regions (e.g., the Horn of Africa [HOA]). This study characterizes meteorological, soil moisture, and hydrological droughts and the propagation from one to the other for 318 catchments in the HOA to improve the understanding of the spatial variability of the drought hazard. We calculate the Standardized Precipitation Index [SPI], Standardized Soil Moisture Index [SSMI], and Standardized Streamflow Index [SSI]. Additionally, we use the variable threshold method to calculate drought duration below a predefined percentile threshold for precipitation, soil moisture, and discharge. The relationship between meteorological, soil moisture, and hydrological drought is examined by finding the SPI accumulation period that shows the highest correlation between SPI and SSMI and SSI timeseries, and by calculating the ratio between the threshold-based precipitation drought duration and soil moisture drought duration, respectively streamflow drought duration. Finally, we investigate the influence of climate and catchment characteristics on these propagation metrics. Results indicate that (1) the propagation from SPI to SSMI and precipitation to soil moisture [P/S/M] mean duration ratio are mainly influenced by soil properties and vegetation, with the short accumulation periods (1-4 months) of SPI found in catchments with cropland, high mean annual precipitation, and low sand and silt content, while longer accumulations (5-7 months) are found in catchments with low upstream mean annual precipitation, and shrub vegetation; (2) the propagation from SPI to SSI and precipitation to streamflow duration ratio are highly influenced by the climate and catchment control, i.e., geology, elevation and land cover, with the short accumulation times in catchments with high annual precipitation, volcanic permeable geology, and cropland, and the longer accumulations in catchments with low annual precipitation, sedimentary rocks and shrubland; and (3) the influence of upstream mean annual precipitation is more important for the propagation from SPI to SSI than from SPI to SSMI. Additionally, precipitation accumulation periods of approximately 1-4 months in wet western areas of HOA, and of approximately 5-7 months in the more dryland regions are found, which is useful information for management because of their more direct relation to impacts.

10

15

20

25

## 1 Introduction

30

There are many droughts in the Horn of Africa [HOA] (including the ongoing multi-year drought) and these have severe impacts such as crop losses, livestock death and diseases, as well as frequent emergencies, food insecurity, infrastructure damages and high economic costs (IGAD & WFP, 2017). This is especially devastating for the small-scale farmers whose livelihood depends on rainfed agricultural systems and livestock (IGAD & WFP, 2017).

35

Soil moisture and hydrological drought, which greatly impact agriculture and water use in ecosystems and society, respectively, are considered to have devastating impacts in the HOA (Shukla and Wood, 2008; Van Loon, 2015). Therefore, it is paramount for water resources management to understand how the drought signal translates from deviating meteorological conditions into soil moisture and finally to hydrological drought. This process is referred to as propagation. Drought propagation is greatly influenced by climate and catchment characteristics (Barker et al., 2016; Van Loon and Laaha, 2015; Van Loon and Van Lanen, 2012). Thus, there is also a need to assess the combined effect of climate and catchment characteristics on drought propagation, for a thorough understanding of the underlying processes of drought development. There are numerous drought propagation studies in data-rich countries (i.e., US, China) but not much has been done for the data-poor regions (i.e., HOA). In this research, we define drought as a prolonged period of below-normal water availability. Drought is normally categorized into three types: meteorological (precipitation deficit), agricultural or soil moisture (soil moisture deficit), and hydrological (abnormally low levels of streamflow in rivers, reservoirs, lakes and groundwater) (He et al., 2013; Huang et al., 2017; Jiang et al., 2019; Van Loon et al., 2016).

45

The frequency, severity and duration of drought are important characteristics of drought events, and can be used to investigate drought propagation. Many studies have quantified these drought characteristics using standardized indices



(i.e., Standardized Precipitation Index [SPI] (Mckee et al., 1993), Standardized Soil Moisture Index [SSMI] (Hao and Aghakouchak, 2014), and Standardized Streamflow Index [SSI] (Huang et al., 2017)). Some studies have also employed threshold-based indices to calculate drought duration and deficit (as a measure of severity) and study drought propagation (Heudorfer and Stahl, 2017; Tallaksen et al., 2009; Van Lanen et al., 2013; Van Loon, 2013; Van Loon et al., 2014; Van Loon and Laaha, 2015). Most of these studies are at catchment scale (Apurv et al., 2017; Huang et al., 2017; Tallaksen et al., 2009) and some at regional scale (Barker et al., 2016; Van Loon, 2013; Van Loon and Laaha, 2015; Xu et al., 2019a). These studies mostly focused on the drought characteristics with some features associated with lagging, attenuation, lengthening and pooling recognized. What is still unclear from these studies is how propagation from precipitation to soil moisture drought relates to climate and catchment characteristics. Moreover, the two approaches to characterize drought differ in that the standardized indices cannot provide information on drought deficit volumes but can be used across different geographical regions as opposed to variable threshold-based method. These methods may provide different information if used for spatial analysis of drought propagation.

Many studies have used statistical methods to assess the drought propagation and relate this to climate and catchment characteristics. Some of the studies provide an indication of which variables to be included in a drought propagation analysis in the HOA, such as geology, landcover, annual mean precipitation and seasonal characteristics. For example, Barker et al. (2016) characterized meteorological and hydrological droughts and their propagation in the UK. The relationship between meteorological and hydrological drought was assessed by cross correlating the 1-month SSI with various SPI accumulation periods using a Pearson correlation coefficient. They also investigated the influence of climate and catchment properties on hydrological drought characteristics and propagation using Pearson correlation together with Spearman's correlation. They found that SPI accumulation periods correlated differently with 1-month SSI depending on the regions in the UK, due to the difference in hydrogeology and mean annual precipitation. Huang et al. (2017) used SPI and SSI to characterize meteorological and hydrological droughts, respectively. They investigated the propagation time and the influence of El Nino Southern Oscillation [ENSO], Artic Oscillation [AO] and underlying surface characteristics on drought propagation in the Wei River Basin in China by using the cross-wavelet analysis. They found that ENSO and AO are strongly correlated with actual evaporation thus, impacted propagation time from meteorological to hydrological drought (which is influenced by seasonal characteristics). Van Loon and Laaha (2014) used variable threshold level methods to characterize meteorological and hydrological drought in 44 Austrian catchments free from major disturbances. They analyzed the combined influence of climate and catchment characteristics of drought propagation using various statistical tools (i.e., bivariate correlation analysis, regression analysis). Their results showed firstly that hydrological drought duration is primarily influenced by storage and release (i.e., base flow index, geology, and land use). Furthermore, the duration of meteorological drought is important for hydrological drought duration. Finally, the hydrological drought deficit is governed by catchment wetness (mean annual precipitation).

These results cannot be easily generalized and applied in the HOA due to its different climate and hydrogeology. Thus, there is still a need for a deeper understanding of the drought propagation in this region and the appropriate indicators to be used for drought characterization. Choosing an appropriate indicator for drought characterization is key to understanding the linkage between the drought hazard and the drought impacts. Different indices may prove valuable depending on the area of application (Vicente-Serrano & Lopez-Moreno, 2005). The objective of this study is to understand (1) how drought characteristics change as the drought propagates from meteorological to soil moisture and finally to hydrological droughts in the HOA; and (2) which climatic and catchment characteristics influence the propagation from meteorological to soil moisture to hydrological drought, using both the standardized and threshold-based indices. The study is conducted on a set of catchments across Kenya, Somalia and Ethiopia with diverse hydro-climatic and landscape conditions.

## 2 Case study area

The study was conducted on a selection of catchments based on level 6 boundaries of HydroBASINS covering Kenya, Somalia and Ethiopia and consisting of 338 catchments (Lehner & Grill, 2013). The region has a seasonal climatological regime. It is mostly semi-arid, but ranges from very humid in the Ethiopian highlands and Mt. Kenya region to very arid in parts of Somalia, southern and southeastern Ethiopia and northeastern Kenya. The region is mostly made up of shrubland with cropland and forests found in the highly wet Ethiopian highlands, around Lake Victoria and the high slopes of Mt. Kenya (Figure 1a). The annual mean precipitation decreases from the east to the west and from high altitude (Ethiopian highlands and Mt. Kenya region experiences annual mean precipitation over



500mm) to low altitude (northeastern Kenya and Somalia experience annual mean precipitation of below 200mm) (Figure 1b and c). The precipitation increases from the Somali coast towards the Kenya coast (Figure 1c), which is also reflected in forest cover (Figure 1a).

The long rains mostly occur during March-May [MAM], while short rains occur in October-December [OND] following the migration of the intertropical convergence zone [ITCZ] from south to north and vice versa (Awange et al., 2016). This is mostly true for Kenya and Somalia, while Ethiopia experiences a single rainy season in June-September [JJAS]. The region also has a very diverse geology ranging from rich volcanic soils in the high slopes of Mt. Kenya and the Ethiopian highlands, to sedimentary rocks in the semi-arid areas of south and southeastern Ethiopia, Somalia, and east and northeastern Kenya (Figure 1d). The diverse topography and seasonality make the region an interesting study area.

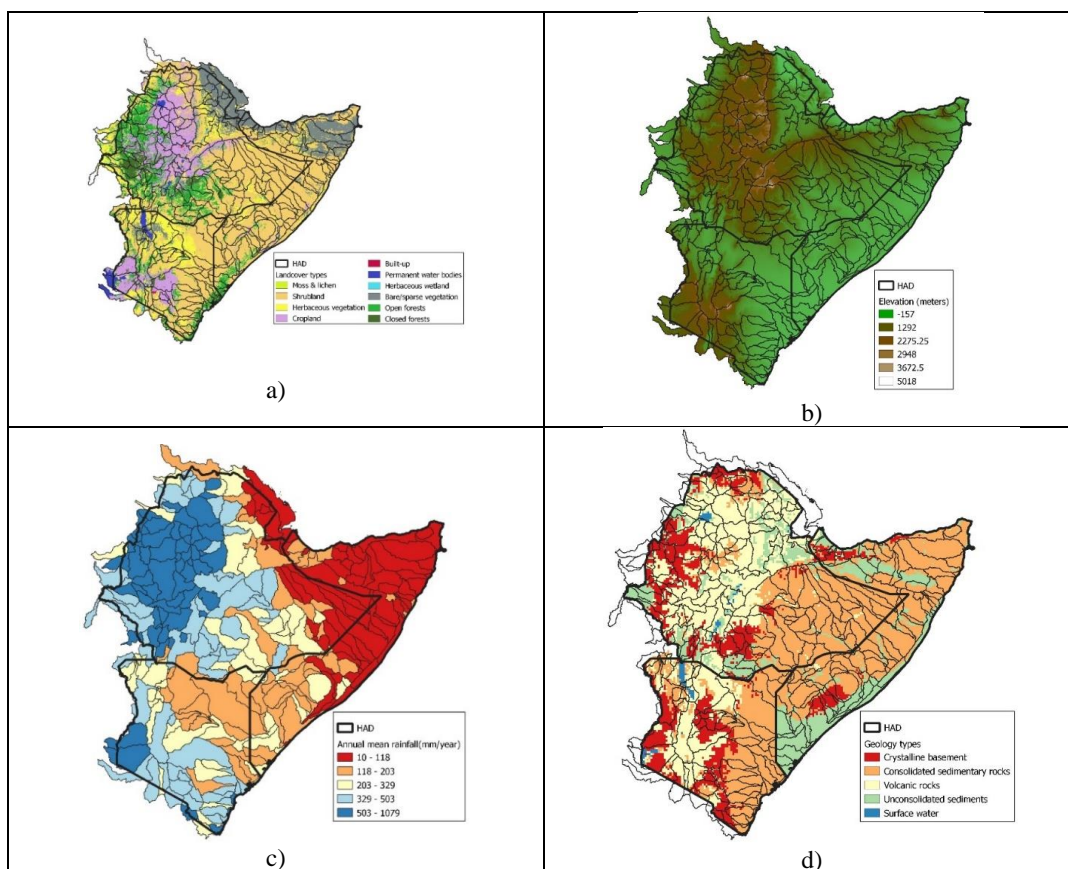
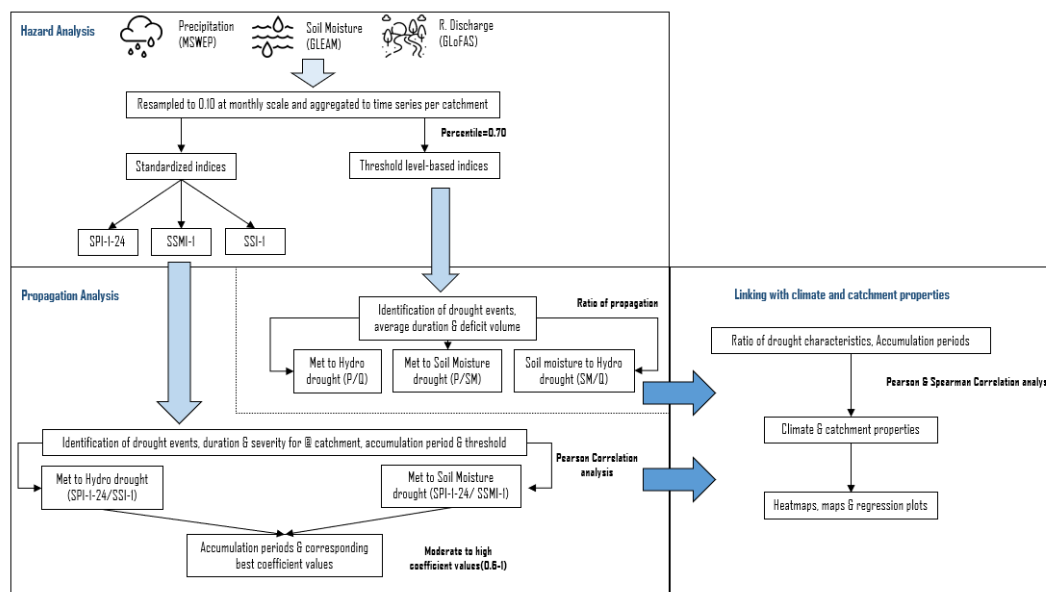


Figure 1: Maps showing some characteristics of the study area: a) landcover (Copernicus) (Buchhorn et al., 2020); b) elevation (STRM) (Farr and Kozbrick, 2000); c) mean annual precipitation (MSWEP) (Beck et al., 2017); and d) geology (Africa Groundwater Atlas, 2022).

### 3 Methodology

The methodology of this study is summarized in Figure 2. First, the data and their respective sources together with the catchment characteristics are discussed (Section 3.1), followed by calculation of the indices (Section 3.2). Second, the drought propagation analysis process is discussed (Section 3.3). Finally, the statistical analysis involving linking of both the standardized and threshold-based indices with the climate and catchment characteristics is discussed (Section 3.4).



120

Figure 2: Detailed methodology framework showing steps taken from hazard analysis to propagation analysis and finally to linking with climate and catchment characteristics.

### 3.1 Data

125 In the past decade, studies have been done in the HOA to understand and characterize extreme events such as droughts. Most of these studies use modelled data due to the lack of observational data in this region. The lack of observational data, especially of streamflow, has led to limited analysis of hydrological drought events. Several of the studies have focused on meteorological and agricultural drought and not hydrological drought (Agutu et al., 2017, 2020; Anderson et al., 2012; Awange et al., 2016; Belal et al., 2014; Dutra et al., 2013; Edossa et al., 2010; Gebrechorkos et al., 2020; Haile et al., 2019, 2020; Kurnik et al., 2011; Lyon, 2014; Nicholson, 2014; Rulinda et al., 2012; Tonini et al., 2012).  
 130 These studies have assessed drought based on soil moisture (model and reanalysis), precipitation (satellite-derived, observed and a combination of both), terrestrial water storage (TWS; through the Gravity Recovery and Climate Experiment) and normalized difference vegetation index (NDVI).

135 In this study we draw upon the same types of datasets as used in previous studies. Ideally, propagation analysis should be based only on observed data but that is not always feasible for large-scale analysis. In this study, we therefore prioritized data sources as closely to observational data as possible, but still covering the entire regional domain of the HOA. Correspondingly, we opted to use reanalysis data for precipitation and soil moisture, but still used modelled data for streamflow as no suitable observational dataset had been found. These gridded datasets are aggregated to catchment resolution based on level 6 hydrological data and maps, HydroSHEDS, (Lehner and Grill, 2013) for catchment delineation. For the analysis, we use the upstream contributing area of each catchment. Catchments with an area of 150km<sup>2</sup> or more were selected for analysis, reducing the number to catchments to 320. A further two catchments are excluded due to missing values (due to the resolution of soil moisture and streamflow datasets) after aggregation at the catchment level, leaving only 318 catchments. The remaining catchments provide good spatial coverage of the HOA and its diverse characteristics.

#### 3.1.1 Hydrometeorological and soil moisture datasets

145 Precipitation data has been retrieved from the Multi-Source Weighted-Ensemble Precipitation [MSWEP] version 1.1. This is a global gridded precipitation (P) dataset that covers the period 1979–present at three hourly temporal and 0.1 degree spatial resolution. It does not contain purely observations but a combination of gauge-, satellite- and reanalysis-based P-estimates, dependent on timescale and location (Beck et al., 2017). This dataset was chosen for this analysis



150 based on its spatial and temporal resolution and good performance in capturing spatial and temporal variation of drought conditions (Xu et al., 2019b).

The soil moisture data has been retrieved from the Global Land Evaporation Amsterdam Model [GLEAM] (version 3.5a). The model applies a set of algorithms to estimate land surface evaporation (also referred to as evapotranspiration) and root zone soil moisture from satellite and reanalysis data at the global scale, with 0.25 degree spatial resolution and daily temporal resolution (Martens et al., 2017; Miralles et al., 2011). It uses the latest version of MSWEP precipitation, (version 2.8), European Space Agency Climate Change Initiative [ESA-CCI] soil moisture (version 5.3), and Vegetation optical depth [VOD] (Martens et al., 2017). The root zone soil moisture is obtained from a multi-layer water balance model that uses precipitation and soil moisture data as inputs. The root zone soil moisture is based on the weighted average of the soil surface of up to 5 cm (topmost layer), which is more variable, and root zone up to 100cm layer. GLEAM datasets have been used in recent studies, including in the Horn of Africa (Javadinejad et al., 2019; Nicolai-Shaw et al., 2017; Peng et al., 2020). For this study, the GLEAM potential evaporation (PET) and root zone soil moisture were used (see <http://www.gleam.eu>) for the period 2010–2020.

Streamflow data has been retrieved from the Global Flood Awareness System [GloFAS] which consists of global gridded river streamflow data, with a horizontal resolution of 0.1 degree at a daily time step and time period of 1979–present (Harrigan et al., 2020). It combines surface and sub-surface runoff from the HTESEL land surface model used within ECMWF’s global atmospheric reanalysis [ERA5] with the LISFLOOD hydrological and channel routing model. LISFLOOD calculates a water balance at a six hourly or daily temporal resolution with 0.05 degree spatial resolution (see <http://www.globalfloods.eu/>). The GloFAS dataset was chosen because of the lack of observational streamflow datasets with sufficient spatial coverage and time period. Additionally, we conducted bias test of GloFAS dataset at specific weather stations in the HAD against observational data. We found that whilst there is a bias, the general variation between the two datasets was similar (see supplementary materials Fig. S1 and S2).

Catchment characteristics were obtained from multiple sources. These sources include BasinATLAS (Linke et al., 2019), upstream annual mean precipitation from MSWEP (Beck et al., 2017), geology types from Africa groundwater atlas (Africa Groundwater Atlas, 2022), and landcover types from Copernicus Global Land Cover layers-Collection 2 (Buchhorn et al., 2020). The catchment characteristics used in this study include soil properties (i.e., percent silt, sand and clay fractions, percent annual mean soil water content), geology types, land cover types, terrain slope, elevation, upstream contributing area, climate zones, upstream annual mean precipitation, global average aridity index, and average population density (further description of these characteristics can be found in Supplementary materials table S1). These catchment characteristics were selected because they have been found in previous studies to influence drought propagation in other regions (Barker et al., 2016; Van Loon, 2013; Van Loon and Laaha, 2015). The characteristics were also selected because drought intensity tends to vary based on the topographic location and time it takes for water to pass through the catchments.

## 3.2 Drought Analysis

### 3.2.1 Standardized indices

The Standardized Precipitation Index [SPI], devised by McKee et al. (1993), allows quantification of precipitation deficits or surpluses on a range of different accumulation periods. The SPI was calculated by summing daily MSWEP precipitation to obtain a monthly temporal resolution. A distribution was fitted through the monthly precipitation values, which was done per watershed to calculate SPI values at accumulation periods of 1 to 24 months. Each watershed within the HOA has a specific distribution which was either normal, gamma, exponential Weibull or lognormal distributions for SPI calculation (Stagge et al., 2015). For Standardized Soil Moisture Index [SSMI] (Ryu and Famiglietti, 2005), we used mean monthly GLEAM rootzone soil moisture content and fitted normal, beta, pearson3 or fisk distributions. For Standardized Streamflow Index [SSI] (Vicente-Serrano et al., 2012) we used mean monthly GloFAS streamflow values and fitted exponential Weibull, lognormal, pearson3 or generalized extreme distributions. The distribution for each catchment and variable was selected based on the Kolmogorov best fit method. Each of these distributions have been proven by previous studies to work for the different indices. The number of zeros in precipitation was taken into consideration following recommendations from Stagge et al. (2015) for SPI. All drought indices were calculated at a monthly resolution for the period 1980–2020.





### 3.2.2 Threshold level-based indices

The threshold-based approach is a drought analysis method that has been employed widely (Heudorfer & Stahl, 2017; Tallaksen et al., 2009; Van Lanen et al., 2013; Van Loon, 2013; Van Loon et al., 2014; Van Loon & Laaha, 2015). Applying this approach, a drought event was defined as any event that falls below the pre-defined threshold. Drought events were identified from the monthly timeseries of the above-mentioned hydrometeorological datasets (precipitation [P], soil moisture [SM] and streamflow [Q] variables) using a monthly-varying threshold-based approach to reflect seasonality. This approach has been previously used in numerous studies (e.g., Beyene et al., 2014; Nyabeze, 2004; Van Huijgevoort et al., 2012; Van Huijgevoort, 2014; Van Loon, 2013; Van Loon et al., 2014; Van Loon & Laaha, 2015; Vidal et al., 2010). The 70<sup>th</sup> percentile was used as threshold. This means that every month of the year has a different threshold level based on the 70<sup>th</sup> percentile of the duration curve of the hydrometeorological variable values in that month, for all the years in the timeseries. In previous studies, percentile ranges between 70<sup>th</sup> and 90<sup>th</sup> have been used (Heudorfer & Stahl, 2017; Van Loon, 2013; Van Loon et al., 2014; Van Loon & Laaha, 2015). After testing different percentile values (70<sup>th</sup>, 80<sup>th</sup> and 90<sup>th</sup> percentiles), we selected the 70<sup>th</sup> percentile because it was able to clearly show the drought propagation from meteorological to hydrological drought. The other percentiles were eliminated because they showed too few droughts and missed most of the major drought years.

The duration of the drought event was determined by the total number of consecutive months that the variable value was below the threshold value. Subsequently, the average drought duration was calculated per catchment in the study area. Finally, the duration ratios were calculated (precipitation drought duration against soil moisture drought duration [P/SM ratio] and streamflow drought duration [P/Q ratio]). A ratio closer to 1 indicates that durations are similar (i.e., not so much clustering of precipitation droughts into streamflow droughts), whereas a ratio closer to 0 indicates there are substantially more precipitation droughts than streamflow droughts, indicating that they have propagated and clustered into less and longer P/Q droughts.

## 3.3 Drought propagation

### 3.3.1 Standardized indices

SSMI and SSI integrate land-surface processes and catchment-scale hydrogeological processes, respectively. Hence, a comparison of SSMI and SSI with the SPI provides an indication of the time taken for the drought signal to propagate through the hydrological cycle from precipitation deficits to soil moisture deficits and finally to streamflow deficits. SPI timeseries with accumulation periods of 1-24 months were cross correlated against SSMI and SSI timeseries using Pearson correlation per catchment. This cross-correlation method has been used in many similar studies (Barker et al., 2016; Huang et al., 2017; Xu et al., 2019a) and can effectively show the similarity between different drought types. The accumulation period with the highest correlation coefficient with either SSMI or SSI was denoted as SPI-*n* and used as an indication of the propagation of drought to soil moisture and streamflow respectively. Only correlation values greater and equal to 0.5 were retained for the analysis of propagation, because these were considered as strong signals.

Propagation times were considered short when the accumulation time of SPI-*n* was below four months. We did not determine whether there was a lag between the SPI and SSI timeseries, because other studies found that strongest correlations are normally at a lag of zero months (i.e., no lag) (Barker et al., 2016). Finally, the catchments were grouped based on the calculated accumulation periods. To check for the independence of data between the catchments based on different groups of accumulation period, a one-way *t*-test was carried out to determine how statistically different the groups are from each other.

### 3.3.2 Threshold based indices

The drought propagation was investigated using duration ratios of the hydrometeorological variables. A ratio of the duration of precipitation droughts against duration of soil moisture droughts was calculated to indicate propagation from precipitation to soil moisture. Furthermore, the ratio of duration of precipitation droughts to streamflow droughts was calculated to show the propagation from precipitation to streamflow. This measurement factors in the effect of meteorological droughts on soil moisture and streamflow droughts leaving only the influence of catchment characteristics.



### 3.4 Influence of possible governing factors of climate and catchment characteristics

245 The effects of climate and catchment characteristics on propagation was investigated by statistical analysis. Firstly,  
we analyzed the strength of the relationships using cross-correlation analysis. We calculated the correlation matrix of  
pairwise combinations of all variables based on Pearson correlation coefficients. As the relationships could be non-  
linear, we also calculated Spearman correlation coefficients and visually inspected the correlation matrix plotted as a  
heatmap to verify the results. We created a clustered heatmap of the Pearson correlation matrix to explore the  
250 intercorrelations of the catchment characteristics. We used the Euclidean distance method to order the coefficients. In  
the Euclidean distance method, rows and columns are arranged according to similarity, hence, making it easier to find  
groups of climate and catchment characteristics with a joint effect on drought propagation. We then plotted individual  
plots for each of the key variables against the propagation indices. Additionally, we used raster zonal statistics in  
QGIS to link variables such as geology, landcover, climate zones, upstream area and elevation to the indices. Secondly,  
255 we performed a one-way *t*-test on the standardized indices clustered catchments. The significance test was used to  
determine whether the cluster of catchments differs per accumulation period.

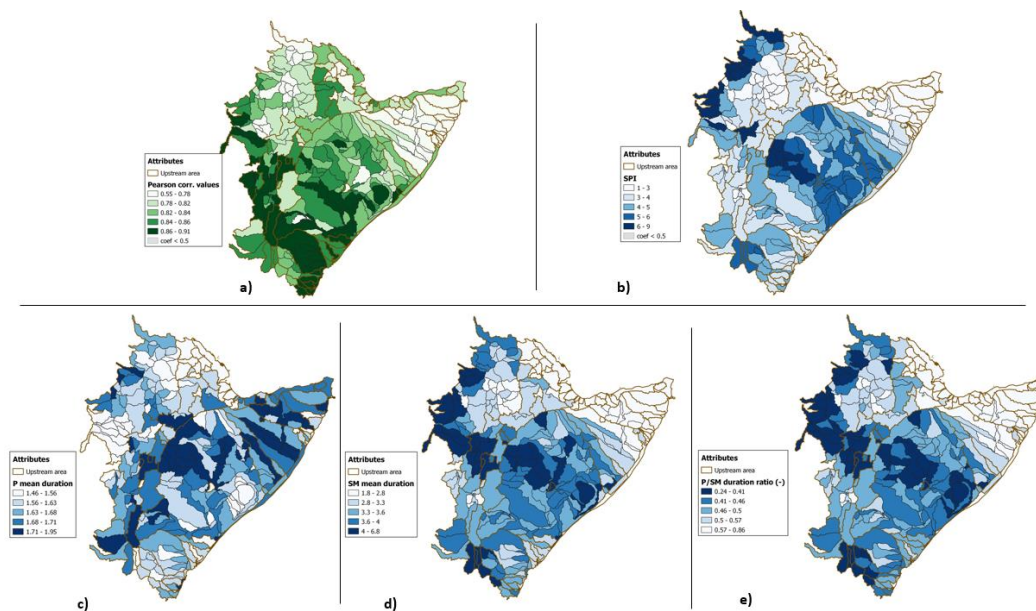
## 4 Results and Discussion

In the following sections, drought propagation and the link with catchment characteristics per propagation indicator  
are discussed in detail. First, the propagation from precipitation to soil moisture drought is presented, followed by the  
260 propagation of soil moisture to discharge drought.

### 4.1 Precipitation to soil moisture

#### 4.1.1 SPI-to-SSMI

The mapping of SPI-*n* for propagation from SPI-to-SSMI (Figure 3a) showed high correlation values in all catchments,  
especially in the south of HOA (Kenya region, average 0.82). The high correlation values were found in the full range  
265 of SPI accumulation periods. This may be due to the strong link between precipitation and soil moisture, since  
GLEAM uses MSWEP precipitation as one of its inputs. The catchments were split equally between the short and  
long accumulation periods (1-4 months and 5-9 months with each 159 catchments (Figure 3b)). The longest  
accumulation periods (9 and 8 months) were located in the northwest of the HAD, with correlation values greater than  
0.7 (Figure 3a). Figure 3b shows that catchments on the northeast coast of the HAD had SPI-*n* between 1 and 3 months,  
270 while those of catchments at the east center were longer (between 5 and 7 months).





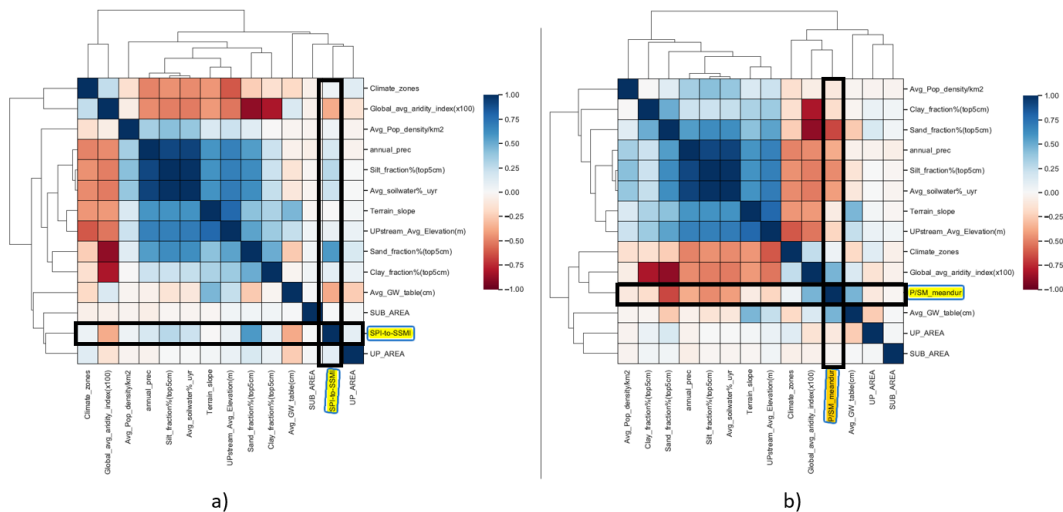
275 *Figure 3: Propagation from precipitation to soil moisture: a) highest coefficient values per catchment (>0.5) from SPI-to-SSMI; b) corresponding SPI-n (SPI accumulation period having highest correlation with SSMI) per catchment; c) mean precipitation drought duration; d) mean soil moisture drought duration; e) ratio of drought mean duration from meteorological to soil moisture (P/S/M).*

### 4.1.2 P/S/M duration ratio

280 The duration of the droughts increases as the drought signal propagates through the hydrological cycle (Figure 3c, and d). The duration of soil moisture droughts is greater than that of precipitation droughts, indicating propagation and clustering of precipitation droughts into soil moisture. The threshold-based drought duration ratio map (P/S/M) (Figure 3e) displays similar processes as the standardized indices propagation map (Figure 3b), i.e., short precipitation to soil moisture response in the northeast (shown by short accumulation periods in the standardized indices and high duration ratio in the threshold indices (P/S/M ratio)).

285 The P/S/M ratio analysis (Figure 3e) shows that the northwest center and northeast center of the HAD have high ratios, meaning in this area soil moisture reacts faster to precipitation (less pooling of the precipitation droughts). The P/S/M ratio decreases moving towards the southeast coast of the HAD (with some catchments having ratios as low as 0.3), which indicates longer soil moisture droughts towards the southeast coast of the HAD. There are also low ratios on the catchments located in the northwest tip and west of the HAD, indicating longer soil moisture droughts and shorter precipitation droughts (Figure 3c and d), meaning the response of soil moisture to precipitation is slower in these catchments (more pooling of the precipitation droughts).

### 4.1.3 Relation of precipitation-to-soil moisture with climate and catchment characteristics



295 *Figure 4: Heatmap of Pearson correlations between the propagation indices and catchment characteristics: a) the SPI-to-SSMI; b) P/S/M mean duration ratio.*

*Note\*. Euclidean distances used for clustering variables with interchangeable correlations. The heatmap based on the Spearman correlation coefficients (see supplementary Figure S4 and S3) showed a similar pattern as Figure 4. Therefore, we assume that linear models (Pearson correlation method) can be used to represent the monotonic relationships even though the relationships are not perfectly linear.*

300 SPI-to-SSMI propagation have longer accumulation periods in catchments with low aridity index and higher sand and low silt fraction (Table 1) and vice versa. These catchments are located in the (semi-)arid east center of the HAD. SPI-to-SSMI propagation also have significant relationships with percent soil water content, and landcover. Similarly, catchments with low P/S/M duration ratio have low aridity index and higher sand fraction (Figure 5a and b). These catchments experience low upstream mean annual precipitation, riddled with shrubland. They correspond to the





305 catchments with slow propagation from precipitation to soil moisture droughts (longer soil moisture droughts; [Figure 3d](#) and medium to longer precipitation droughts; [Figure 3c](#)) due to slow reaction of soil moisture to precipitation. The slow reaction occurs because the soil tends to be very dry in these areas, hence the process of wetting of the soil surface occurs first before infiltration can begin. Additionally, SPI-to-SSMI propagation have longer accumulation in catchments with closed and open forests, and herbaceous wetland and vegetation ([Table 1](#)). In these catchments, the interaction of precipitation with soil moisture is slow leading to the weaker correlations ([Figure 3a](#)). This phenomenon is consistent with findings of previous studies (e.g., [Sehler et al., 2019](#)), which claimed that landcover, soil moisture and precipitation have stronger correlations in (semi-)arid regions with limited vegetation, while weaker correlations are found in humid regions with forests and densely vegetated. SPI-to-SSMI propagation have shorter accumulation periods and P/SM duration ratios are high in catchments with cropland and bare or sparse vegetation; these catchments are found in the northwest center (Ethiopian highlands) and northeast tip, respectively.

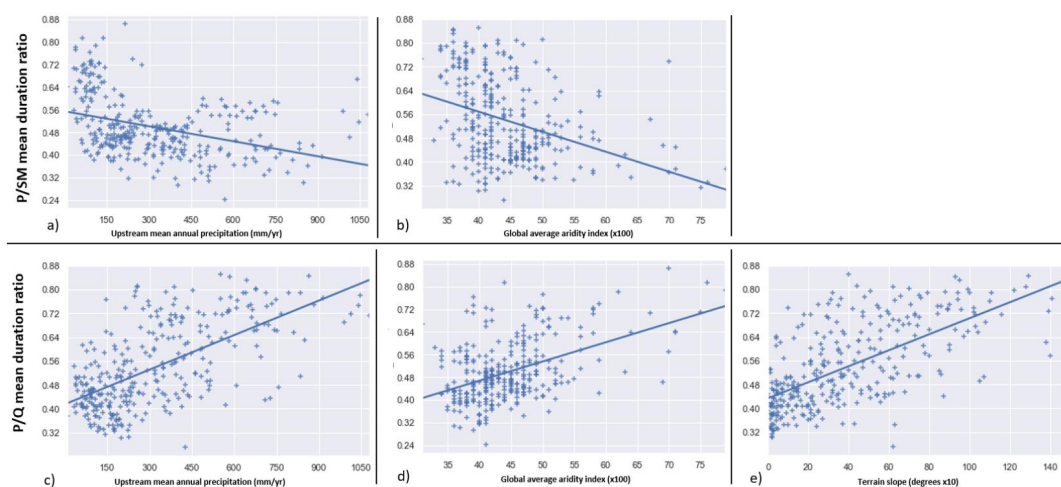


Figure 5: Catchment characteristics against P/SM and P/Q mean duration ratios.

320 The propagation time from precipitation to soil moisture is also influenced by precipitation variability, however this influence is not pronounced in both SPI-to-SSMI propagation and P/SM mean duration ratio. This is seen in the low positive correlation value between upstream mean annual precipitation and SPI-*n* for SPI-to-SSMI ([Figure 4](#)), the average distribution of the accumulation periods per equal interval (quantile) grouping of the upstream mean annual precipitation ([Table 1](#)), and the less steep slope (highest value 0.56) in P/SM mean duration ratio against upstream mean annual precipitation ([Figure 5a](#)). This weak correlation can be explained because both the short and long accumulation periods ([Figure 3b](#)) and the low and high P/SM mean duration ratios ([Figure 3e](#)) can be found in the catchments located in wetter western part of HAD ([Figure 1c](#)). P/SM ratio decrease with increasing upstream mean annual precipitation, meaning most catchments with high P/SM ratios located in the wet west of the HAD were fast responding, whereas ones with high P/SM ratios found in the east of the HAD slow responding. SPI-to-SSMI propagation and P/SM mean duration ratio have no dependence on the upstream area, elevation, and geology type (equal distribution of the mean in [Table 1](#)) (see supplementary material [Table S2](#) and [S3](#)).

Table 1: Mean average accumulation period per upstream mean annual precipitation, upstream elevation, upstream area, geology type, and landcover type ( $\leq 4$  months are considered short accumulation periods and  $\geq 5$  long accumulation periods).

	Precipitation (mm)	SPI-to-SSMI (months)	SPI-to-SSI (months)		Elevation (m)	SPI-to-SSMI (months)	SPI-to-SSI (months)
Upstream mean annual precipitation	10-118	6.0	3.4	Upstream elevation	3-402	3.9	6.0
	118-203	5.9	2.7		402-731	4.4	6.0
	203-329	4.9	2.0		732-1043	4.7	4.9
	329-503	4.8	1.4		1044-1544	5.1	4.8



	<b>503-1079</b>	3.1	1.0		<b>1545-2493</b>	4.3	3.1
	<i>Area (km<sup>2</sup>)</i>				<i>Geology type</i>		
Upstream Area (km <sup>2</sup> )	<b>152-3935</b>	4.3	5.6	Geology Type	<b>Crystalline basement</b>	5.0	3.8
	<b>3935-7259</b>	4.1	5.5		<b>Consolidated sedimentary rocks</b>	4.4	5.0
	<b>7259-15257</b>	5.0	5.4		<b>Volcanic rocks</b>	4.3	3.1
	<b>15257-47890</b>	4.3	4.4		<b>Unconsolidated sediments</b>	4.4	4.4
	<b>47890-745375</b>	4.7	4.2		<b>Surface water</b>	4.0	1.7
		<i>Sand fraction</i>				<i>Landcover types</i>	
Percent sand fraction (%)	<b>11-26</b>	3.1	5.5	Landcover types	<b>Shrubland</b>	4.8	4.8
	<b>26-29</b>	4.4	5.6		<b>Herbaceous vegetation</b>	4.6	4.2
	<b>29-32</b>	4.8	5.1		<b>Cropland</b>	4.4	2.8
	<b>32-35</b>	5.1	4.0		<b>Built-up</b>	4.6	3.5
	<b>35-40</b>	5.8	4.6		<b>Herbaceous wetland</b>	4.8	2.9
						<b>Bare/sparse vegetation</b>	2.3
					<b>Open forests</b>	5.3	3.8
					<b>Closed forests</b>	5.0	2.7

335 In conclusion, SPI-to-SSMI propagation and P/SM mean duration is more dependent on the soil properties, landcover and when it last rained. All these variables are linked to the storage capacity of the catchment. We see that catchments with high percent sandy soils and shrubland have longer reaction times and long durations, while catchments with low percent sandy soils and cropland have short reaction times and shorter durations. This link with soil properties is in line with findings from Van Loon and Laaha (2014), who showed that factors such as storage in soils, aquifers, and lakes influence drought duration with longer durations in larger storage and shorter durations in smaller storage.

## 340 4.2 Precipitation to streamflow

### 4.2.1 SPI-to-SSI

345 The SPI-to-SSI analysis (Figure 6a) shows that the catchments with the low correlation values were mostly found in the northwest at the center around the Ethiopian highlands. These areas in the northwest center also have short accumulation periods (Figure 6c). A few catchments in the northwest tip have longer accumulation periods (5 to 7 months). The majority of the catchments had long accumulation periods ( $\leq 5$  months; 212 catchments), with 106 catchments having short accumulation periods ( $\geq 4$  months). The signal strength decreases the further it moves down the hydrological cycle, with the highest correlation value in SPI-to-SSMI being 0.91 and 0.77 for SPI-to-SSI (Figure 3a and Figure 6a, respectively). This becomes clear by the number of catchments where the strength of the correlation value is less than 0.5 (grey sub-catchments in Figure 6a and c). This leads to fewer catchments with correlation values higher than 0.5 as the drought propagates from meteorological to soil moisture and finally to streamflow drought.

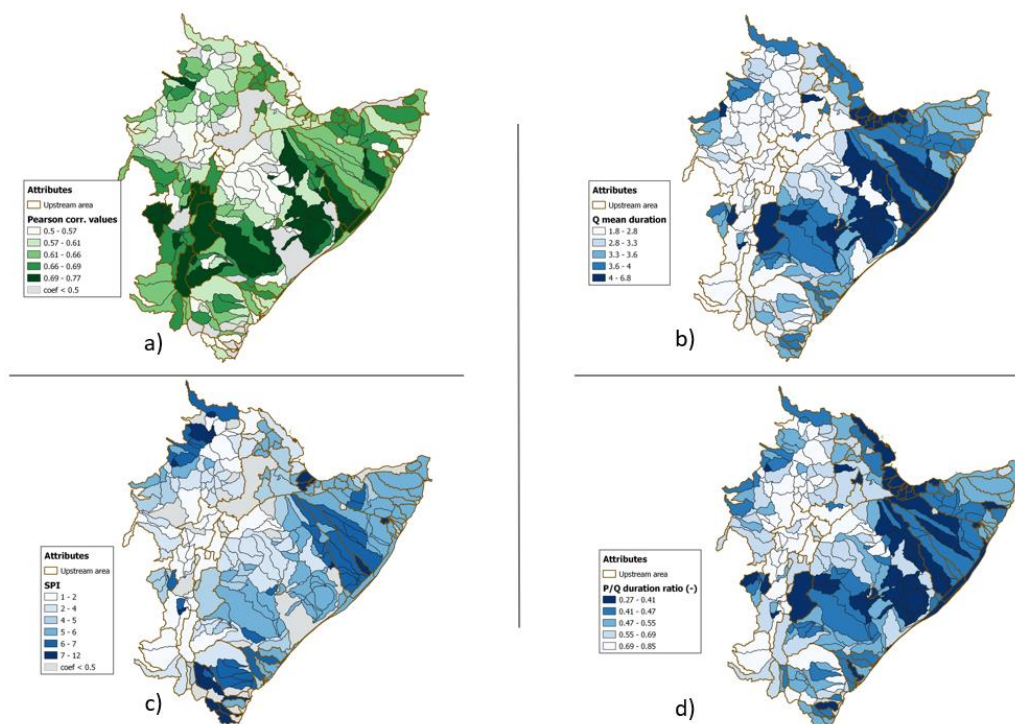


Figure 6: Propagation from precipitation to streamflow: a) Highest coefficient values per catchment ( $>0.5$ ) from SPI-to-SSI; b) mean streamflow drought duration; c) corresponding SPI-n (SPI accumulation period having highest correlation with SSI) per catchment; d) ratio of drought mean duration from meteorological to streamflow (P/Q).

#### 355 4.2.2 P/Q mean duration ratio

P/Q mean duration ratio analysis (Figure 6d) shows that the highest duration ratios are found in the catchments in the west and southwest of the HAD and low ratios in the east of the HAD towards the coast. The catchments with the high P/Q mean duration ratios experience short streamflow droughts and longer precipitation droughts as shown in Figure 6b and Figure 3c, respectively. In these locations, the response of runoff when it rains is fast as opposed to the catchments having low duration ratios and experiencing longer streamflow droughts, however the streamflow droughts are still longer than precipitation droughts. Streamflow droughts are shorter and there is less clustering of precipitation droughts to soil moisture and finally streamflow droughts in the west and southwest as opposed to the east towards the coast where they become longer and with increased clustering. The catchments in the east of the HAD are also located within the arid and semi-arid areas, therefore, whenever it rains, the process of infiltrations has to occur first before any runoff is produced, making the response of streamflow to precipitation longer. The threshold-based drought duration ratio map (P/Q) (Figure 6d) displays similar processes as the standardized indices propagation map (Figure 6c), i.e., short precipitation to streamflow response in the west (shown by short accumulation periods in the standardized indices and high duration ratio in the threshold indices P/Q ratio).

#### 370 4.2.3 Relation of precipitation to streamflow with climate and catchment characteristics

Propagation from precipitation to streamflow is influenced by catchment-scale hydrogeological properties. SPI-to-SSI propagation and P/Q mean duration ratio have longer accumulation periods and longer duration droughts, respectively, in catchments with sedimentary rock structure, shrubland, bare or spare vegetation, low upstream mean annual precipitation, high aridity, low elevation, medium percent silt fraction and low percent sand fraction. These catchments are located in the east of the HOA towards the coast (Figure 6c and d) and associated with small to big catchment upstream areas (Table 1). The influence of upstream area on propagation was not as pronounced as we expected (Table



1 and Figure 7). The lack of influence of upstream areas on the propagation of drought from precipitation to streamflow contradicts the findings in previous studies (Haslinger et al., 2014; Van Lanen et al., 2013; Van Loon & Laaha, 2015; Vidal et al., 2010), suggesting that the propagation time from meteorological drought to hydrological drought may be aggravated by basin size. In these catchments, streamflow mean duration (Figure 6b) shows longer time scales than the precipitation mean duration (Figure 3c), which reflects the propagation, indicating pooling of shorter precipitation drought events into longer and fewer streamflow drought events due to catchment storage processes. The catchments streamflow response to precipitation was slower, hence, longer accumulation periods and low P/Q mean ratios. This is caused by other processes in these areas, such as infiltration and wetting of the soil surface, that need to first occur before the process of runoff. Catchments with short accumulation periods and high P/Q mean duration ratios have high upstream mean annual precipitation, low aridity, volcanic soils, cropland, forests and high elevation (Table 1 and Figure 5). These catchments streamflow responses to precipitation are faster because of the high saturation of the soils, which are mostly located in the west of HOA. These findings are in line with previous studies (e.g., Li et al. 2019, Laizé & Hannah, 2010), that found that propagation time from meteorological drought to hydrological drought depends on the flow concentration time which is highly affected by elevation, slope, percentage arable land and bedrock permeability.

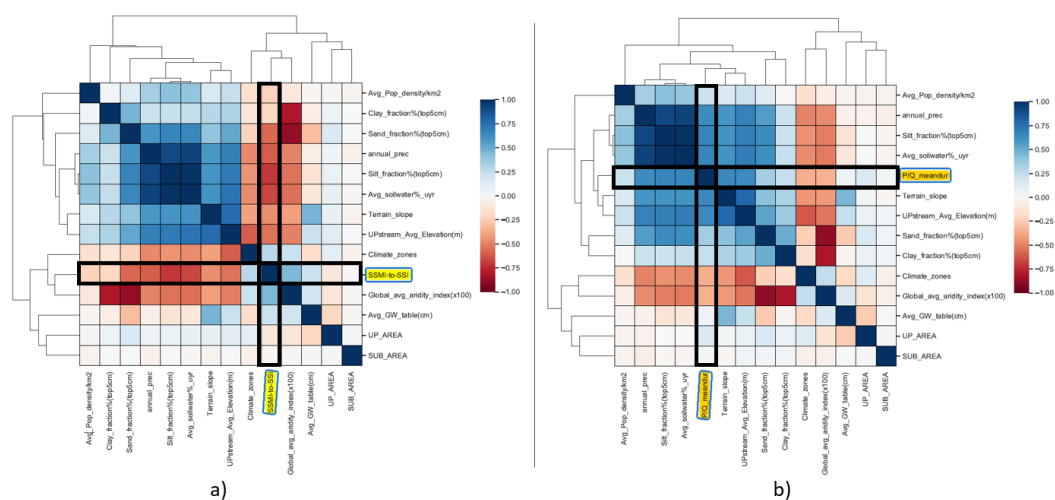


Figure 7: Heatmap of Pearson correlations between the propagation indices and catchment characteristics: a) the SPI-to-SSI; b) P/Q mean duration ratio. Euclidean distances used for clustering variables with interchangeable correlations.

395 The differences in catchments in both SPI-to-SSI propagation and P/Q mean duration ratio has a spatial pattern that strongly reflect the heterogeneity of the geology (Figure 1d), landcover (Figure 1a) and the precipitation gradient (Figure 1c) from the wetter west to the drier east of the HOA. The catchments general precipitation climate is much more important in influencing propagation from SPI-to-SSI and P/Q mean duration ratio as opposed to propagation from precipitation to soil moisture (Table 1 and Figure 5a). The strong link may be a result of the prominent precipitation gradient between the wet and (semi-)arid areas. Rainfall in the semi-arid areas is highly erratic and the dry spells last for longer periods, leading to very low storage (Vicente-Serrano & Lopez-Moreno, 2006) and longer propagation durations, which translates to longer droughts. This finding is in accordance with Van Loon et al., (2014) and Barker et. al. (2016), who identified that seasonality in precipitation is a major climatic factor affecting drought propagation from meteorological to hydrological droughts.

405 Additionally, the correlation value of upstream mean annual precipitation in SPI-to-SSI propagation was lower when compared to terrain slope, percent silt fraction, upstream average elevation and percent average annual soil water content (Figure 7). This shows that in the propagation from precipitation to streamflow, the catchment properties related to soil properties, geology and landcover are more influential than upstream annual mean precipitation in determining the drought propagation. This result is in line with Barker et. al. (2016), who found that the hydrological drought characteristics of catchments with permeable aquifer outcrops had a weak correlation with mean annual



precipitation and a strong correlation with catchment storage characteristics such as Base Flow Index (BFI) or percentage of highly fractured rock.

## 5 Discussion

### 5.1 Implications for research

415 When comparing our results with catchment-scale studies (see Section 4), we find comparable drought propagation  
processes and a similar influence of climate and catchment characteristics on this propagation. As a study specific for  
the HOA region, our results have a number of important implications for drought risk analysis in dryland areas, but  
may not be valid for other regions. The HOA was chosen because of the large variability in climate and catchment  
characteristics. Within the study region, the precipitation can be found to be related to the elevation (increasing  
420 precipitation with increase in altitude and increasing aridity towards the east, which also has decreasing altitude and  
precipitation). When comparing catchments within the dryland region of the study area, we learn that catchment-scale  
hydrogeological processes, such as geology and landcover, are dominant in influencing propagation from precipitation  
to streamflow, while land surface processes, for example soil properties, influence the propagation from precipitation  
to soil moisture (Figure 3). This is in accordance with previous studies (e.g., Barker et al., 2016; Van Loon, 2013).

425 We find differences in propagation from precipitation to soil moisture to also be influenced by precipitation variability,  
with the humid west part of HOA having catchments with both short and long propagation timescales and the drier  
east center having only long propagation timescales. We have learned that drought periods in the catchments in the  
humid west of the HOA (with higher global average aridity index, fertile volcanic soils, and cropland) are shorter than  
in the catchments in the (semi-)arid east of the HOA. For instance, the catchments in the (semi-)arid east with  
430 shrubland, bare or sparse vegetation and underlain with sedimentary rocks (consolidate and unconsolidated) are  
affected by longer periods of soil moisture. In addition, streamflow drought and the timescale for the propagation from  
meteorological drought to soil moisture drought to hydrological drought is also longer ( $\geq 5$  months). Therefore, for the  
process of drought propagation from precipitation to streamflow, it is important to monitor not only precipitation  
forecasts but information on hydrogeological characteristics, such as geology and landcover, of the catchment is also  
435 essential. Incorporating this knowledge in hydrological drought forecasting could significantly increase predictive  
value of forecasting systems by making the forecast less dependent on the forecasting skill of actual precipitation. We  
also confirmed that drought duration is influenced by both climate and catchment control processes, similar to Van  
Loon and Laaha, (2014). There is still a need to further investigate the effect on the propagation timescale when we  
include groundwater.

440 The research also highlights some of the issues with using SPI, SSMI, SSI, and threshold-based duration ratios. The  
nature of standardized indices makes it unable to identify regions with high seasonal climates and arid regions (Hayes  
et al., 1999). It fails to capture the water deficit amounts in the different catchments and regions that are more prone  
to drought than others, as opposed to the threshold-based indices. Additionally, misleading large positive and negative  
values may occur in the arid regions with the short accumulation periods (1, 2 or 3 months). Although calculating the  
445 SPI, SSMI or SSI for any user-defined accumulation periods makes the indicators more flexible, it remains important  
that meaningful accumulation periods are chosen to capture the drought conditions and also to select appropriate  
indicators (Vicente-Serrano & Lopez-Moreno, 2005). Furthermore, the results confirm that accumulation periods  
should be selected based on drought impacts. The threshold-based indices represent the specific drought event  
duration, hereby better representing the link with catchment characteristics and better capturing seasonal precipitation  
450 variability.

Based on the results presented in this paper, we provide an argument for considering terrestrial processes on the  
drought propagation in the context of drought risk analysis. We found that drought propagation from meteorological  
to soil moisture and to hydrological drought cannot be explained by atmospheric processes alone. The propagation  
process is highly influenced by climate and catchment characteristics, hence, when forecasting droughts it is preferred  
455 to use a full hydrological model framework, or at least an indicator-based method which takes (either implicitly or  
explicitly) such characteristics into consideration, as the results of our study suggests.





## 5.2 Implications for drought monitoring and early warning

460 Drought mitigation and water resource management require reliable and efficient drought monitoring and early  
warning systems (M&EW), as they are a critical component of drought preparedness (Barker et al., 2016; Safavi et  
al., 2018). The efficiency of these systems in analyzing extremes is highly determined by the choice of indices which  
must consider and integrate different aspects of information. Drought M&EW systems usually use standardized  
indices such as the SPI, especially since the SPI is the most widely used index to characterize drought (Vicente-  
Serrano & Lopez-Moreno, 2005). However, the use of standardized indices and threshold-based indices is not  
465 widespread and not well developed for soil moisture and hydrological droughts in the HOA. For example, the National  
Drought Monitoring Agency (NDMA) in Kenya has a good drought M&EW system, however this uses only  
precipitation, while impacts are more likely to be associated with soil moisture and hydrological droughts. The SSI  
and the use of threshold-based indices are less common in the HOA. This may be due to the lack of streamflow data  
in this region compared to precipitation data, especially for the short timescales required to produce useful drought  
470 M&EW products. However, monitoring soil moisture and hydrological variables and incorporating such indices is  
beneficial for reliable and effective drought planning and water resource management, and it is especially useful for  
communication purposes if precipitation, soil moisture and streamflow are monitored in a comparable manner.

While the use of streamflow and soil moisture data directly in drought M&EW systems is preferred, these systems  
cannot be used due to lack of data in this region. Therefore, the SPI could provide a surrogate for soil moisture and  
475 streamflow impacts, provided suitable propagation times are known. This also ensures the use of standardized indices  
in the HOA and discourages the use of threshold-based indices (which require raw data), and considering the  
uncertainty in modelled and reanalysis data, it is better to standardize the datasets as standardized indices do (Van  
Loon & Laaha, 2014; Van Lanen et al., 2013; Van Loon, 2013). The correlation results (Figure 3b and Figure 6c)  
showing the spatial variability of SPI- $n$  (the accumulation period that is strongly correlated with SSMI-1 and SSI-1,  
480 respectively), provide an indication of accumulation periods that could serve as a proxy for soil moisture droughts or  
streamflow droughts in the monthly precipitation data. This allows the use of precipitation data, which are more readily  
available, for identifying future potential soil moisture and streamflow droughts. Additionally, the short soil moisture  
and streamflow droughts that have been more influential for the drought planning and water resource management are  
better captured by the short accumulation periods (Figure 3b and Figure 6c), which are less affected by the decreasing  
485 long-term precipitation and streamflow trends in the east of the HOA and increasing trends in the west of the HOA  
(Gebrechorkos et al., 2020). Water managers can use this information on soil moisture and streamflow trends to see  
when to start controlling the water users and anticipate drought impacts. The obtained results may also be applicable  
in water resource forecasting.

## 5.3 Recommendations and further research

490 Groundwater plays an important role in mitigating the impacts of drought and as a source of water supply in arid and  
semi-arid areas, particularly in the east of the HOA (Adloff et al., 2022). Therefore, to fully understand the process of  
drought propagation, it is necessary to include the groundwater component in the analysis. Moreover, while storage  
in the catchment plays a key role in determining the duration of drought and propagation, it is also important to take  
into account seasonality and autocorrelation of soil moisture and also streamflow caused by infiltration and  
495 evaporation. Therefore, undertaking propagation analysis through the hydrological cycle and including the  
groundwater component would provide a more comprehensive picture and assessment of the influence of climate and  
catchment characteristics on the drought duration, severity and propagation. In addition, the effect of seasonal  
variability (based on the long and the short rains) in drought propagation should be further investigated. Seasonal  
variability is particularly important for the propagation from precipitation-to-soil moisture especially in the west of  
500 the HOA where the response of soil moisture is dependent on when it last rained. Similarly, the timing of hydrological  
droughts leading to impacts should be investigated.

Finally, for observation-based studies of drought, the availability of hydrological records is a limitation. This is  
particularly true for the HOA. The period of analysis (1980-2020) does not capture the full range of hydrological  
variability. We assume that longer records could influence the accumulation periods presented here, although the same  
505 regional picture and propagation characteristics would probably emerge. Furthermore, the use of modelled and  
reanalysis data introduced some uncertainty into the analysis. For example, the GloFAS streamflow dataset was  
developed for a global application and represents streamflow in perennial systems typical of humid regions.  
Correspondingly, it does not represent ephemeral flow processes typical of dryland regions. As such, the dataset tends



510 to overestimate the streamflow in arid and semi-arid areas. As such, the dataset tends to overestimate streamflow in  
arid and semi-arid areas. Hence, a modelling framework that is suitable for dryland regions, where hydrological  
processes are distinct from humid regions, would be preferred. For example, a model like DRYP hydrological model  
(Quichimbo et al., 2021) has been designed specifically for dryland hydrological processes such as ephemeral flow,  
surface-groundwater interactions, and high-resolution rainfall - as such has a good potential for further investigation  
and application. This model has been used to investigate the role of gridded rainfall resolution into societally-relevant  
515 water stores (streamflow, soil moisture and groundwater recharge) (Quichimbo et al., submitted) and has been used  
to generate water balance forecasts based on seasonal climate forecasts in the HOA (MacLeod et al., in review). A  
regional version of this model would provide a better alternative for follow-up studies given the GloFAS dataset  
limitations .

## 6 Conclusion

520 Drought propagation from meteorological to soil moisture to hydrological drought in 318 catchments in the HOA was  
analyzed using standardized indices (over a range of accumulation periods) and threshold-based indices (drought-  
duration ratios). In addition, the influence of possible governing factors, such as climate and catchment characteristics,  
was also investigated. The research shows that:

- 525 • Precipitation to soil moisture propagation time is longer (5-7 months) in catchments with shrubland, closed  
and open forests, herbaceous wetland and vegetation, and high sand and low silt fraction, while being shorter  
(2-4 months) in catchments with cropland and high upstream mean annual precipitation.
- Precipitation to streamflow propagation time is longer in catchments with sedimentary rock structure, low  
mean annual precipitation, and shrubland, while being shorter in catchments with volcanic soils, high annual  
mean precipitation, cropland and forests.
- 530 • In precipitation to streamflow propagation the catchment properties related to soil properties, geology,  
elevation and landcover are more influential than upstream annual mean precipitation. However, the upstream  
mean annual precipitation is more important for streamflow drought duration, severity and propagation from  
precipitation-to-streamflow as opposed to propagation from precipitation to soil moisture.

535 In summary, precipitation to soil moisture propagation is more dependent on the soil properties as opposed to the  
hydrogeological characteristics (i.e., elevation) while the precipitation to streamflow propagation experience the  
combined effect of climate and catchment control properties (i.e., elevation, geology). The results in this study provide  
an indication of precipitation accumulation periods that could serve as a proxy for soil moisture and streamflow  
droughts in the HOA. The precipitation accumulation periods of roughly 1-4 months in wet western areas of HOA,  
540 and of roughly 5-7 months in the more dryland regions are the most suitable for drought analysis. These results can  
be used as a foundation for future developments in drought monitoring and early warning systems in the HOA, laying  
foundations for better drought preparedness and increased resilience to drought and its impacts in water resources.

**Acknowledgements.** This study is an outcome of the Down2Earth Project (D2E). An EU Horizon 2020 Project  
funded under grant agreement number 869550. We thank Marthe Wens, PhD researcher at the Institute of  
Environmental Studies, Vrije Universiteit Amsterdam for help with python scripts. The authors would like to thank  
545 Bristol Principal Investigator on D2E Katerina Michaelides, Associate Professor at the University of Bristol, UK, for  
her constructive comments that helped improve the paper.

**Competing interests.** The authors have no competing interests to declare.

## 7 References

- 550 Adloff, M., Singer, M. B., MacLeod, D. A., Michaelides, K., Mehrnegar, N., Hansford, E., Funk, C., and Mitchell,  
D.: Sustained Water Storage in Horn of Africa Drylands Dominated by Seasonal Rainfall Extremes, *Geophys.*  
*Res. Lett.*, 49, e2022GL099299, <https://doi.org/10.1029/2022GL099299>, 2022.
- Agutu, N. O., Awange, J. L., Zerihun, A., Ndehedehe, C. E., Kuhn, M., and Fukuda, Y.: Assessing multi-satellite  
remote sensing, reanalysis, and land surface models' products in characterizing agricultural drought in East  
Africa, *Remote Sens. Environ.*, 194, 287–302, <https://doi.org/10.1016/j.rse.2017.03.041>, 2017.



- 555 Agutu, N. O., Awange, J. L., Ndehedehe, C., and Mwaniki, M.: Consistency of agricultural drought characterization over Upper Greater Horn of Africa (1982–2013): Topographical, gauge density, and model forcing influence., *Sci. Total Environ.*, 709, <https://doi.org/10.1016/j.scitotenv.2019.135149>, 2020.
- Anderson, C. L., Biscaye, P., Harris, K. P., Merfeld, J., and Reynolds, T.: Proxy errors with policy consequences : How common crop yield measures can bias estimates of management-based agricultural productivity gains, 1–13, 2012.
- 560
- Apurv, T., Sivapalan, M., and Cai, X.: Understanding the Role of Climate Characteristics in Drought Propagation, *Water Resour. Res.*, 53, 9304–9329, <https://doi.org/10.1002/2017WR021445>, 2017.
- Awange, J. L., Khandu, Schumacher, M., Forootan, E., and Heck, B.: Exploring hydro-meteorological drought patterns over the Greater Horn of Africa (1979–2014) using remote sensing and reanalysis products, *Adv. Water Resour.*, 94, 45–59, <https://doi.org/10.1016/j.advwatres.2016.04.005>, 2016.
- 565
- Barker, L. J., Hannaford, J., Chiverton, A., and Svensson, C.: From meteorological to hydrological drought using standardised indicators, *Hydrol. Earth Syst. Sci.*, 20, 2483–2505, <https://doi.org/10.5194/hess-20-2483-2016>, 2016.
- Beck, H. E., Van Dijk, A. I. J. M., Levizzani, V., Schellekens, J., Miralles, D. G., Martens, B., and De Roo, A.: MSWEP: 3-hourly 0.25° global gridded precipitation (1979–2015) by merging gauge, satellite, and reanalysis data, *Hydrol. Earth Syst. Sci.*, 21, 589–615, <https://doi.org/10.5194/hess-21-589-2017>, 2017.
- 570
- Belal, A. A., El-Ramady, H. R., Mohamed, E. S., and Saleh, A. M.: Drought risk assessment using remote sensing and GIS techniques, *Arab. J. Geosci.*, 7, 35–53, <https://doi.org/10.1007/s12517-012-0707-2>, 2014.
- Beyene, B., Van Loon, A. F., Lanen, H. V., and Torfs, P.: Investigation of variable threshold level approaches for hydrological drought identification, *Hydrol. Earth Syst. Sci. Discuss.*, 11, 12765–12797, <https://doi.org/10.5194/HESSD-11-12765-2014>, 2014.
- 575
- Africa Groundwater Atlas: <https://www2.bgs.ac.uk/africagroundwateratlas/downloadGIS.html>, last access: 17 October 2022.
- Buchhorn, M., Smets, B., Bertels, L., De Roo, B., Lesiv, M., Tsendbazar, N. E., Linlin, L., and Tarko, A.: Copernicus Global Land Service: Land Cover 100m: Version 3 Globe 2015–2019, Geneva, Switzerland, 2020.
- 580
- Dutra, E., Magnusson, L., Wetterhall, F., Cloke, H. L., Balsamo, G., Boussetta, S., and Pappenberger, F.: The 2010–2011 drought in the Horn of Africa in ECMWF reanalysis and seasonal forecast products, *Int. J. Climatol.*, 33, 1720–1729, <https://doi.org/10.1002/joc.3545>, 2013.
- Edossa, D. C., Babel, M. S., and Gupta, A. D.: Drought analysis in the Awash River Basin, Ethiopia, *Water Resour. Manag.*, 24, 1441–1460, <https://doi.org/10.1007/s11269-009-9508-0>, 2010.
- 585
- Farr, T. G. and Kobrick, M.: Shuttle Radar Topography Mission produces a wealth of data, *AGU*, 81, 503–503, 2000.
- Gebrechorkos, S. H., Hülsmann, S., and Bernhofer, C.: Analysis of climate variability and droughts in East Africa using high-resolution climate data products, *Glob. Planet. Change*, 186, 103130, <https://doi.org/10.1016/j.gloplacha.2020.103130>, 2020.
- 590
- Haile, G. G., Tang, Q., Sun, S., Huang, Z., Zhang, X., and Liu, X.: Droughts in East Africa: Causes, impacts and resilience, *Earth-Sci. Rev.*, 193, 146–161, <https://doi.org/10.1016/j.earscirev.2019.04.015>, 2019.
- Haile, G. G., Tang, Q., Leng, G., Jia, G., Wang, J., Cai, D., Sun, S., Baniya, B., and Zhang, Q.: Long-term spatiotemporal variation of drought patterns over the Greater Horn of Africa, *Sci. Total Environ.*, 704, <https://doi.org/10.1016/j.scitotenv.2019.135299>, 2020.



- 595 Hao, Z. and Aghakouchak, A.: A Nonparametric Multivariate Multi-Index Drought Monitoring Framework, *J. Hydrometeorol.*, 15, <https://doi.org/10.1175/JHM-D-12-0160.1>, 2014.
- Harrigan, S., Zsoter, E., Alfieri, L., Prudhomme, C., Salamon, P., Barnard, C., Cloke, H., and Pappenberger, F.: GloFAS-ERA5 operational global river discharge reanalysis 1979 present, GloFAS-ERA5 Oper. Glob. River Disch. Reanalysis 1979- Present, 1–23, <https://doi.org/10.5194/essd-2019-232>, 2020.
- 600 Haslinger, K., Koffler, D., Schöner, W., and Laaha, G.: Exploring the link between meteorological drought and streamflow: Effects of climate-catchment interaction, *Water Resour. Res.*, 50, 2468–2487, <https://doi.org/10.1002/2013WR015051>, 2014.
- Hayes, M. J., Svoboda, M. D., Wihite, D. A., and Vanyarkho, O. V.: Monitoring the 1996 Drought Using the Standardized Precipitation Index, *Bull. Am. Meteorol. Soc.*, 80, 429–438, [https://doi.org/10.1175/1520-0477\(1999\)080<0429:MTDUTS>2.0.CO;2](https://doi.org/10.1175/1520-0477(1999)080<0429:MTDUTS>2.0.CO;2), 1999.
- 605 He, B., Wu, J., Lü, A., Cui, X., Zhou, L., Liu, M., and Zhao, L.: Quantitative assessment and spatial characteristic analysis of agricultural drought risk in China, *Nat. Hazards*, 66, 155–166, <https://doi.org/10.1007/s11069-012-0398-8>, 2013.
- Heudorfer, B. and Stahl, K.: Comparison of different threshold level methods for drought propagation analysis in Germany, *Hydrol. Res.*, 1311–1326, <https://doi.org/10.2166/nh.2016.258>, 2017.
- 610 Huang, S., Li, P., Huang, Q., Leng, G., Hou, B., and Ma, L.: The propagation from meteorological to hydrological drought and its potential influence factors, *J. Hydrol.*, 547, 184–195, <https://doi.org/10.1016/j.jhydrol.2017.01.041>, 2017.
- IGAD Climate Prediction & Application Centre, (ICPAC)/ World Food Programme (WFP): Greater Horn of Africa Climate Risk and Food Security Atlas, Nairobi, 2017.
- 615 Javadinejad, S., Hannah, D., Ostad-Ali-Askari, K., Krause, S., Zalewski, M., and Boogaard, F.: The Impact of Future Climate Change and Human Activities on Hydro-climatological Drought, Analysis and Projections: Using CMIP5 Climate Model Simulations, *Water Conserv. Sci. Eng.*, 4, 71–88, <https://doi.org/10.1007/s41101-019-00069-2>, 2019.
- 620 Jiang, S., Wang, M., Ren, L., Xu, C., Yuan, F., Liu, Y., Lu, Y., and Shen, H.: A framework for quantifying the impacts of climate change and human activities on hydrological drought in a semiarid basin of Northern China, *Hydrol. Process.*, 33, 1075–1088, <https://doi.org/10.1002/hyp.13386>, 2019.
- Kurnik, B., Barbosa, P., and Vogt, J.: Testing two different precipitation datasets to compute the standardized precipitation index over the horn of Africa, *Int. J. Remote Sens.*, 32, 5947–5964, <https://doi.org/10.1080/01431161.2010.499380>, 2011.
- 625 Lehner, B. and Grill, G.: Global river hydrography and network routing: baseline data and new approaches to study the world’s large river systems, *Wiley Online Libr.*, 2171–2186, <https://doi.org/10.1002/hyp.9740>, 2013.
- Li, Q., He, P., He, Y., Han, X., Zeng, T., Lu, G., and Wang, H.: Investigation to the relation between meteorological drought and hydrological drought in the upper Shaying River Basin using wavelet analysis, <https://doi.org/10.1016/j.atmosres.2019.104743>, 2019.
- 630 Linke, S., Lehner, B., Ouellet Dallaire, C., Ariwi, J., Grill, G., Anand, M., Beames, P., Burchard-Levine, V., Maxwell, S., Moidu, H., Tan, F., and Thieme, M.: Global hydro-environmental sub-basin and river reach characteristics at high spatial resolution, 6, <https://doi.org/10.1038/s41597-019-0300-6>, 2019.
- Lyon, B.: Seasonal drought in the Greater Horn of Africa and its recent increase during the March-May long rains, *J. Clim.*, 27, 7953–7975, <https://doi.org/10.1175/JCLI-D-13-00459.1>, 2014.
- 635



- MacLeod, D.A., Quichimbo, A.E., Michaelides, K., Asfaw, D., Rosolem, R., Cuthbert, M.O., Otenyo, E., Segele, Z., Rigby, R., Otieno, G., Hassaballah, K., Tadege, A., Singer, M.B. (revision in review) Translating seasonal climate forecasts into water balance forecasts for decision making. *PLOS Climate*.
- 640 Martens, B., Miralles, D. G., Lievens, H., Van Der Schalie, R., De Jeu, R. A. M., Fernández-Prieto, D., Beck, H. E., Dorigo, W. A., and Verhoest, N. E. C.: GLEAM v3: Satellite-based land evaporation and root-zone soil moisture, *Geosci. Model Dev.*, 10, 1903–1925, <https://doi.org/10.5194/gmd-10-1903-2017>, 2017.
- Mckee, T. B., Doesken, N. J., and Kleist, J.: THE RELATIONSHIP OF DROUGHT FREQUENCY AND DURATION TO TIME SCALES, *Eighth Conf. Appl. Climatol.*, 17–22, 1993.
- 645 Miralles, D. G., Holmes, T. R. H., De Jeu, R. A. M., Gash, J. H., Meesters, A. G. C. A., and Dolman, A. J.: Global land-surface evaporation estimated from satellite-based observations, *Hydrol. Earth Syst. Sci.*, 15, 453–469, <https://doi.org/10.5194/hess-15-453-2011>, 2011.
- Nicholson, S. E.: A detailed look at the recent drought situation in the Greater Horn of Africa, *J. Arid Environ.*, 103, 71–79, <https://doi.org/10.1016/j.jaridenv.2013.12.003>, 2014.
- 650 Nicolai-Shaw, N., Zscheischler, J., Hirschi, M., Gudmundsson, L., and Seneviratne, S. I.: A drought event composite analysis using satellite remote-sensing based soil moisture, *Remote Sens. Environ.*, 203, 216–225, <https://doi.org/10.1016/j.rse.2017.06.014>, 2017.
- Nyabeze, W. R.: Estimating and interpreting hydrological drought indices using a selected catchment in Zimbabwe, *Phys. Chem. Earth Parts ABC*, 29, 1173–1180, <https://doi.org/10.1016/j.pce.2004.09.018>, 2004.
- 655 Peng, J., Dadson, S., Hirpa, F., Dyer, E., Lees, T., Miralles, D. G., Vicente-Serrano, S. M., and Funk, C.: A pan-African high-resolution drought index dataset, *Earth Syst. Sci. Data*, 12, 753–769, <https://doi.org/10.5194/essd-12-753-2020>, 2020.
- Quichimbo, E. A., Singer, M. B., Michaelides, K., Hobley, D. E. J., Rosolem, R., and Cuthbert, M. O.: DRYP 1.0: a parsimonious hydrological model of DRYland Partitioning of the water balance, *Geosci. Model Dev.*, 14, 6893–6917, <https://doi.org/10.5194/gmd-14-6893-2021>, 2021.
- 660 Quichimbo, E. A., Singer, M.B., Michaelides, K., Rosolem, R., MacLeod, D.A., Asfaw, D., Cuthbert M.O. (submitted) Assessing the sensitivity of modelled water partitioning to global precipitation datasets in data-scarce dryland regions.
- Rulinda, C. M., Dilo, A., Bijker, W., and Stein, A.: Characterising and quantifying vegetative drought in East Africa using fuzzy modelling and NDVI data, *J. Arid Environ.*, 78, 169–178, <https://doi.org/10.1016/j.jaridenv.2011.11.016>, 2012.
- 665 Ryu, D. and Famiglietti, J. S.: Characterization of footprint-scale surface soil moisture variability using Gaussian and beta distribution functions during the Southern Great Plains 1997 (SGP97) hydrology experiment, *Water Resour. Res.*, 41, <https://doi.org/10.1029/2004WR003835>, 2005.
- 670 Safavi, H. R., Raghbi, V., Mazdiyasi, O., and Mortazavi-Naeini, M.: A new hybrid drought-monitoring framework based on nonparametric standardized indicators, *Hydrol. Res.*, 49, 222–236, <https://doi.org/10.2166/nh.2017.266>, 2018.
- Sehler, R., Li, J., Reager, J., and Ye, H.: Investigating Relationship Between Soil Moisture and Precipitation Globally Using Remote Sensing Observations, *J. Contemp. Water Res. Educ.*, 168, 106–118, <https://doi.org/10.1111/j.1936-704x.2019.03324.x>, 2019.
- 675 Shukla, S. and Wood, A. W.: Use of a standardized runoff index for characterizing hydrologic drought, *Geophys. Res. Lett.*, 35, 1–7, <https://doi.org/10.1029/2007GL032487>, 2008.





- Stagge, J. H., Kohn, I., Tallaksen, L. M., and Stahl, K.: Modeling drought impact occurrence based on meteorological drought indices in Europe, *J. Hydrol.*, 530, 37–50, <https://doi.org/10.1016/j.jhydrol.2015.09.039>, 2015.
- 680 Tallaksen, L. M., Hisdal, H., and Van Lanen, H. A. J.: Space-time modelling of catchment scale drought characteristics, *J. Hydrol.*, 375, 10, <https://doi.org/10.1016/j.jhydrol.2009.06.032>, 2009.
- Tonini, F., Lasinio, G. J., and Hochmair, H. H.: Mapping return levels of absolute NDVI variations for the assessment of drought risk in Ethiopia, *Int. J. Appl. Earth Obs. Geoinformation*, 18, 564–572, <https://doi.org/10.1016/j.jag.2012.03.018>, 2012.
- 685 Van Huijgevoort, M. H. J., Hazenberg, P., Van Lanen, H. A. J., and Uijlenhoet, R.: A generic method for hydrological drought identification across different climate regions, *Hydrol. Earth Syst. Sci.*, 16, 2437–2451, <https://doi.org/10.5194/hess-16-2437-2012>, 2012.
- Van Huijgevoort, M. V.: Hydrological drought : characterisation and representation in large-scale models, (*Thesis*) 2014.
- 690 Van Lanen, H. A. J., Wanders, N., Tallaksen, L. M., and Van Loon, A. F.: Hydrological drought across the world: impact of climate and physical catchment structure, *Hydrol. Earth Syst. Sci.*, 17, 1715–1732, <https://doi.org/10.5194/hess-17-1715-2013>, 2013.
- Van Loon, A. F.: How climate and catchment characteristics influence hydrological drought development and recovery, (*Thesis*), 2013.
- 695 Van Loon, A. F.: Hydrological drought explained, *Wiley Interdiscip. Rev. Water*, 2, 359–392, <https://doi.org/10.1002/wat2.1085>, 2015.
- Van Loon, A. F. and Laaha, G.: Hydrological drought severity explained by climate and catchment characteristics, *J. Hydrol.*, 526, 3–14, <https://doi.org/10.1016/J.JHYDROL.2014.10.059>, 2015.
- Van Loon, A. F. and Van Lanen, H. A. J.: A process-based typology of hydrological drought, *Hydrol Earth Syst Sci*, 16, 1915–1946, <https://doi.org/10.5194/hess-16-1915-2012>, 2012.
- 700 Van Loon, A. F., Tjeldeman, E., Wanders, N., Van Lanen, H. A. J., Teuling, A. J., and Uijlenhoet, R.: How climate seasonality modifies drought duration and deficit, *J. Geophys. Res. Atmospheres*, 119, 4640–4656, <https://doi.org/10.1002/2013JD020383>, 2014.
- 705 Van Loon, A. F., Stahl, K., Di Baldassarre, G., Clark, J., Rangelcroft, S., Wanders, N., Gleeson, T., Van Dijk, A. I. J. M., Tallaksen, L. M., Hannaford, J., Uijlenhoet, R., Teuling, A. J., Hannah, D. M., Sheffield, J., Svoboda, M., Verbeiren, B., Wagener, T., and Van Lanen, H. A. J.: Drought in a human-modified world: Reframing drought definitions, understanding, and analysis approaches, *Hydrol. Earth Syst. Sci.*, 20, 3631–3650, <https://doi.org/10.5194/hess-20-3631-2016>, 2016.
- 710 Vicente-Serrano, S. M. and Lopez-Moreno, J. I.: Hydrological response to different time scales of climatological drought: an evaluation of the Standardized Precipitation Index in a mountainous Mediterranean basin, *Hydrol. Earth Syst. Sci.*, 11, 2005.
- Vicente-Serrano, S. M. and Lopez-Moreno, J. I.: THE INFLUENCE OF ATMOSPHERIC CIRCULATION AT DIFFERENT SPATIAL SCALES ON WINTER DROUGHT VARIABILITY THROUGH A SEMI-ARID CLIMATIC GRADIENT IN NORTHEAST SPAIN, *Int. J. Climatol.*, 26(11), 1427–1453, <https://doi.org/10.1002/joc.1387>, 2006.
- 715 Vicente-Serrano, S. M., López-Moreno, J. I., Beguería, S., Lorenzo-Lacruz, J., Azorin-Molina, C., and Morán-Tejeda, E.: Accurate Computation of a Streamflow Drought Index, *J. Hydrol. Eng.*, 17, 318–332, [https://doi.org/10.1061/\(ASCE\)HE.1943-5584.0000433](https://doi.org/10.1061/(ASCE)HE.1943-5584.0000433), 2012.



- 720 Vidal, J.-P., Martin, E., Franchistéguy, L., Habets, F., Soubeyrou, J.-M., Blanchard, M., and Baillon, M.: Multilevel and multiscale drought reanalysis over France with the Safran-Isba-Modcou hydrometeorological suite, *Hydrol. Earth Syst. Sci.*, 14, 459–478, <https://doi.org/10.5194/hess-14-459-2010>, 2010.
- Xu, Y., Zhang, X., Wang, X., Hao, Z., Singh, V. P., and Hao, F.: Propagation from meteorological drought to hydrological drought under the impact of human activities: A case study in northern China, <https://doi.org/10.1016/j.jhydrol.2019.124147>, 2019a.
- 725 Xu, Z., Wu, Z., He, H., Wu, X., Zhou, J., Zhang, Y., and Guo, X.: Evaluating the accuracy of MSWEP V2.1 and its performance for drought monitoring over mainland China, *Atmospheric Res.*, 226, 17–31, <https://doi.org/10.1016/j.atmosres.2019.04.008>, 2019b.